Rahal OUARED [1], Morsli SEBAA[2], Tayeb ALLAOUI[3], Mouloud DENAI[4], Amina TAMER[5]

Laboratory of Electrical and Computer Engineering ,university of Tiaret, Algeria (1,2,3,5)
School of Engineering &Computer Science, University of Hertfordshire, UK, (4)

Improved Control Strategy of a Shunt Active Power Filter Using an adaptive fuzzy direct distorting power control and an adaptive fuzzy logic controller

Abstract. An increase in residential, commercial, and industrial non-linear loads connected to the power distribution network results in non-sinusoidal currents generation. These currents cause the appearance of harmonics to alter the operation of electrical equipment, reduce network performance and cause component damage. The most solution to these problems is the use of Shunt Active Power Filter (SAPF). The purpose of this paper is the design of an adaptive Fuzzy logic Direct distorting Power Control (AFL-DDPC) to attenuate the harmonic effect. This control method is known to reduce the fluctuations of the active and reactive powers at low speeds in contrast to the classical approach, where the frequency of switching is uncontrollable. Furthermore, an adaptive fuzzy logic PI controller (AFLC-PI) controls the DC-link capacitor voltage for the compensation performance of the APF to improve the quality of the electric currents. Simulations results of the SAPF are presented to compare the performance of the proposed and the classical control approaches.

*Streszczenie. Wzrost nieliniowych odbiorników mieszkaniowych, handlowych i przemysłowych podłączonych do sieci rozdzielczej powoduje powstawanie prądów niesinusoidalnych. Prądy te powodują pojawienie się harmonicznych, które zmieniają działanie sprzętu elektrycznego, zmniejszają wydajność sieci i powodują uszkodzenia komponentów. Najlepszym rozwiązaniem tych problemów jest zastosowanie Shunt Active Power Filter (SAPF). Celem tego artykułu jest zaprojektowanie adaptacyjnego sterowania mocą z bezpośrednim zniekształceniem w logice rozmytej (AFL-DDPC) w celu złagodzenia efektu harmonicznego. Wiadomo, że ten sposób sterowania zmniejsza fluktuacje mocy czynnej i biernej przy niskich prędkościach, w przeciwieństwie do klasycznego podejścia, w którym częstotliwość przełączania jest niekontrolowana. Ponadto adaptacyjny sterownik PI z logiką rozmytą (AFLC-PI) steruje napięciem kondensatora obwodu DC w celu kompensacji wydajności APF w celu poprawy jakości prądów elektrycznych. Przedstawiono wyniki symulacji SAPF w celu porównania wydajności proponowanego i klasycznego podejścia do sterowania. (**Udoskonalona strategia sterowania bocznikowego filtra mocy aktywnej Wykorzystanie adaptacyjnego sterowania mocą rozmytego bezpośredniego zniekształcenia i adaptacyjnego sterownika logiki rozmytej**)*

Keywords: HActive power filter, Fuzzy Logic Controller, adaptive Fuzzy logic PI Control
Słowa kluczowe: Filtr mocy HActive, sterownik logiki Fuzzy, adaptacyjna logika Fuzzy PI Control

Introduction

It is not enough to produce electrical energy. Its quality, as well as its routing, are currently one of the main concerns of energy suppliers and organizations specialized in electrical energy quality. Among the causes of the deterioration in the quality of the electrical network is harmonic pollution, which has become very widespread. The most well-known effects of this phenomenon include capacitor deterioration, circuit breaker tripping at inopportune times, resonance problems with network elements, heating of the neutral conductor and transformer, etc. In comparison with a classical solution means, such as over-sizing of installations or passive filtering. Network specialists consider active filtering to be the advanced solution for filtering harmonics. This solution can adapt to changes in the load and the electrical network without affecting the electrical installation supplier and consumer [1].

The active filter contains electronic modules advanced enough to analyze the signal at the input of a load and inject the harmonics present, but with reverse polarity. Mainly, active filters are used to clean the network and keep the THD according to the standard used to regulate the control of harmonic distortions. The general principle of the active filter is to inject into the network a harmonic signal of the same amplitude but in phase opposition with those absorbed by the load. Thus, the current absorbed in the electrical grid will be sinusoidal. Therefore, it is necessary to identify precisely the harmonic currents of the pollutant load [2], [3].

By dint of fully controllable semiconductor components, active filtering has been the subject of numerous research studies to compensate for these harmonic currents generated by the polluting charges connected to the electrical networks [4], [5].In addition,a considerable amount of literature has been published on active filter control. Rahmani et al. in [6] propose a combined system of a thyristor-controlled reactor and a shunt hybrid power filter. Also, Patjosh et al. in [7] present a control scheme that adopted the voltage source inverter to decrease current harmonics generated by the nonlinear load. Man et al. in [8] implement a single-phase active shunt filter using sliding mode control. Furthermore, extensive research has been doing in the fuzzy logic active filter control, like doing by Benyettou et al. I in [9], Loutfi et al. in [10], Bhende et al. in [11], and Mikkili et al. in [12].

This work aims to develop efficient and advanced control techniques such as fuzzy logic for harmonics cleaning. Therefore, to expose the necessary elements constituting the power part of the SAFP which are, the regulation of the DC bus voltage, the control algorithm used to identify the references of currents or voltages, the loop for regulating the voltage of the capacitive tank, the control mode used for the generation of power switch control orders. The aim is to improve the characteristics of the filtering while using a control method of reduced complexity.

The remaining paper is organized as follows: Section 2 presents the modeling of the SAPF-FCI circuit and the SRF algorithm to extract the reference currents. Section 3 explains the operating principle of the FCI and shows the control of flying capacitor voltage and the regulation of the DC bus voltage. In Section 4, the current loop controllers are derived. The simulation results obtained are discussed in Section 5.

System Configuration

The system under study, shown in Figure 1, comprises a three-phase source, two series filters (Rs, Ls) and (Rc, Lc). The whole system supply inductive load via AC/DC converter. Furthermore, a parallel active filter with DC-link via DC/AC inverter is used to enhance the quality of the network.
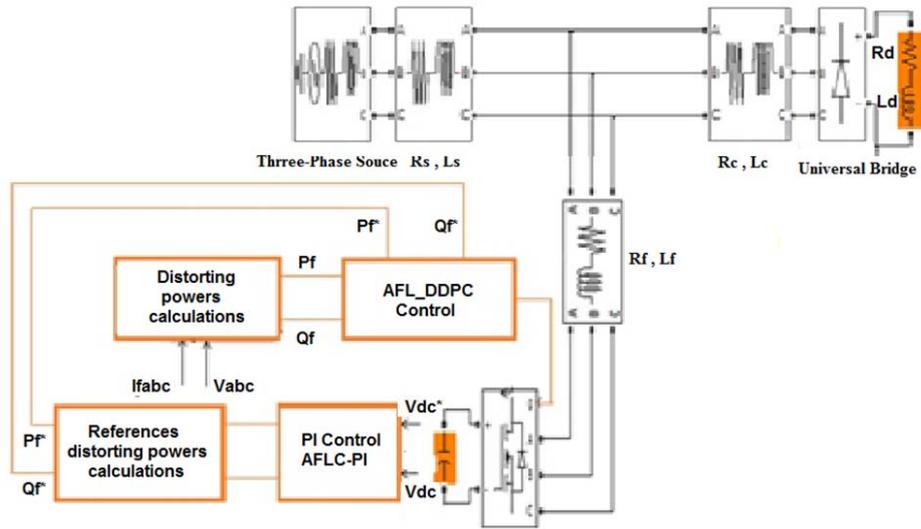
Fig.1. The system configuration

The different controls AFL-DDPC, PI control AFLC-PI are used to control this filter

Since all home appliances are AC loads, a DC-AC inverter regulated at 220 V with frequency of 60Hz is used.

Modeling of the system

The instantaneous distorting active and reactive powers can be estimated without measuring the network voltages. The expressions allowing this estimation are based on the measurement of the harmonic currents, the measurement of the DC bus voltage, and the states of the switches are given as follows [13].

$$(1)\ P_f = \left(L_f \frac{di_{fa}}{dt} + L_f \frac{di_{fb}}{dt} + L_f \frac{di_{fc}}{dt} \right) + v_{dc} \left(s_a i_{fa} + s_b i_{fb} + s_c i_{fc} \right)$$

$$(2)\ Q_f = \sqrt{3L_f} \left(\frac{di_{fa}}{dt} i_c - \frac{di_{fc}}{dt} i_{fa} \right) -$$

$$\frac{1}{\sqrt{3}} v_{dc} \left[s_a \left(i_{fb} - i_{fc} \right) + s_b \left(i_{fc} - i_{fa} \right) + s_c \left(i_{fb} - i_{fc} \right) \right]$$

The transformation of three-phase voltages and currents in the α-β frame is given by the following expressions:

$$(3)\ \begin{bmatrix} V_\alpha \\ V_\beta \end{bmatrix} = \sqrt{\frac{2}{3}} \begin{bmatrix} 1 & \frac{-1}{2} & \frac{-1}{2} \\ 0 & \frac{\sqrt{2}}{2} & -\frac{\sqrt{2}}{2} \end{bmatrix} \begin{bmatrix} V_a \\ V_b \\ V_c \end{bmatrix}$$

$$(4)\ \begin{bmatrix} I_\alpha \\ I_\beta \end{bmatrix} = \sqrt{\frac{2}{3}} \begin{bmatrix} 1 & \frac{-1}{2} & \frac{-1}{2} \\ 0 & \frac{\sqrt{2}}{2} & -\frac{\sqrt{2}}{2} \end{bmatrix} \begin{bmatrix} I_a \\ I_b \\ I_c \end{bmatrix}$$

The instantaneous distorting active power P_f and the instantaneous distorting reactive power Q_f are defined by [14]:

$$(5)\ \begin{bmatrix} P_f \\ Q_f \end{bmatrix} = \begin{bmatrix} V\alpha & V\beta \\ -V\beta & V\alpha \end{bmatrix} \begin{bmatrix} I_\alpha \\ I_\beta \end{bmatrix}$$

Control strategies

The SAFP control configuration in this work comprises two parts, one part an adaptive Fuzzy logic Direct distorting Power Control (AFL-DDPC) for the extraction of harmonic. The second part is the control of the DC link by a PI adaptive fuzzy logic controller (PI-AFLC) for the compensation performance of the APF to improve the quality of the electric currents.

An adaptive Fuzzy logic Direct distorting Power Control (AFL-DDPC)

This work uses a new technique based on the direct control of distorting power DDPC to ensure the active filtering of harmonic currents. This technique is similar to the classical DPC, but it is based on calculating the references of the distorting active and reactive powers. The active SAFP filter can be controlled from the distorting power control loops. In this technique, there are no harmonic current control loops and no PWM block [15]. A switching table determines the switching states of the static converter based on the instantaneous errors between the actual and estimated values of the distorting active and reactive powers. The active Pf and reactive Qf distorting powers are estimated from harmonic voltage and current measurements compared to their references Pf* and Qf*, respectively.

The Pf* reference is provided by the product between the current, the output of the DC voltage regulator, and the DC voltage. In contrast, the Qf* reference is set to zero to achieve a unity power factor. Instantaneous errors between actual and estimated distorting powers are controlled directly with hysteresis controllers and a look-up table. The error signals Sp and Sq and the phase angle of voltage tata are supplied to the switching table (Table 1), which stores Sa, Sb, and Sc of the converter. Optimal switching states are selected such that power errors are kept within the hysteresis bands. For this purpose, the stationary coordinates are divided into 12 sectors, as shown in Figure 2, and the sectors can be expressed as follow [15], [16]:

$$(6)\ \theta = artg \left(\frac{V_\beta}{V_\alpha} \right)$$

Table 1. The parameters of the sensor

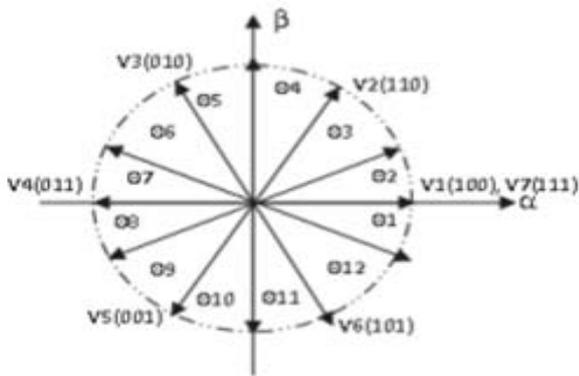| S_p	S_q	Θ_1	Θ_2	Θ_3	Θ_4	Θ_5	Θ_6	Θ_7	Θ_8	Θ_9	Θ_{10}	Θ_{11}	Θ_{12}
1	0	V_6	V_7	V_1	V_0	V_2	V_7	V_3	V_0	V_4	V_7	V_5	V_0
	1	V_7	V_7	V_0	V_0	V_7	V_7	V_0	V_0	V_7	V_7	V_0	V_0
0	0	V_6	V_1	V_1	V_2	V_2	V_3	V_3	V_4	V_4	V_5	V_5	V_6
	1	V_1	V_2	V_2	V_3	V_3	V_4	V_4	V_5	V_5	V_6	V_6	V_1

Fig.2. Sectors and vectors of SAFP.

According to the different possible combinations of these three states, eight voltage vectors can be applied to the input of the rectifier: two null vectors (v_0 and v_7) and six non-zero vectors (v_1, v_2, v_3, v_4, v_5, v_6). These vectors are represented in the α-β stationary coordinate system, as shown in Figure 1. The six non-zero vectors divide the α-β plane into six sectors, each of which is divided into two equal sectors, to obtain precise control. The reference tracking errors of the active and reactive distorting powers, introduced into two-level hysteresis comparators, make it possible to establish two logic outputs Sp and Sq, which take the state "1" for an increase in the controlled variable (Pf or Qf) and the state "0" for a decrease: [17], [18]:

$$(11) \quad \begin{aligned} &if \ \ P_f^* - P_f \geq H_p \Rightarrow S_p = 1 \\ &if \ \ P_f^* - P_f \leq H_p \Rightarrow S_p = 0 \\ &if \ \ Q_f^* - Q_f \geq H_p \Rightarrow S_q = 1 \\ &if \ \ Q_f^* - Q_f \leq H_p \Rightarrow S_q = 0 \end{aligned}$$

An adaptive fuzzy direct distorting power control

The proposed adaptive fuzzy logic direct distorting power control (AFL-DDPC) shown in figure 3.
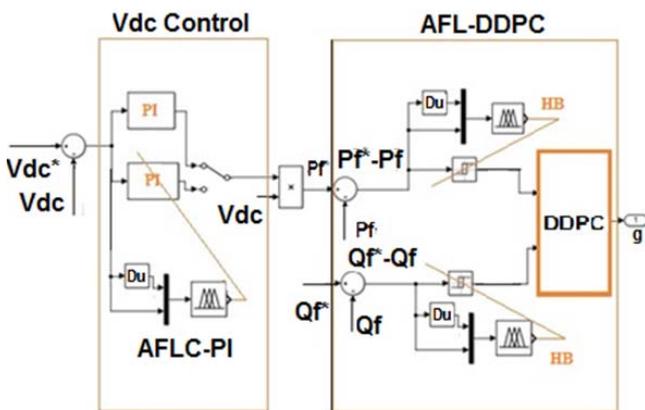
Fig.3. The proposed structure of an adaptive fuzzy logic direct distorting power.

In this proposed technique, the switching signal for the voltage source inverter will be generated by the adaptive hysteresis band. The hysteresis band value is implemented with a fuzzy logic controller (FLC). The inputs to the FLC are the errors of real and reactive distorting powers (epf, eqf) and the variation of these errors (depf, deqf), and the output of the FLC is the hysteresis band HB.

The memberships functions of the inputs variables are shown in figures 4 and 5. With seven fuzzy sets for error labeled negative very large NTG, negative large NG,

negative medium NM, zero EZ, positive medium PM, large positive PG, positive very large PTG. For error variation, NG is negative large, NM is negative medium, EZ is zero, PM is positive medium, and PG is positive large. for Vs(t)

For the output variable HB, very very small TTS, very small TS, small S, medium M, large L, very large TL and very very large TTL. The resulting inference rules are listed in Table 2.
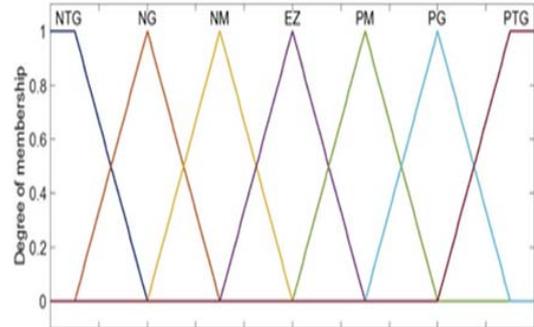
Fig.4. Member ship functions for error of the real and reactive distorting powers.
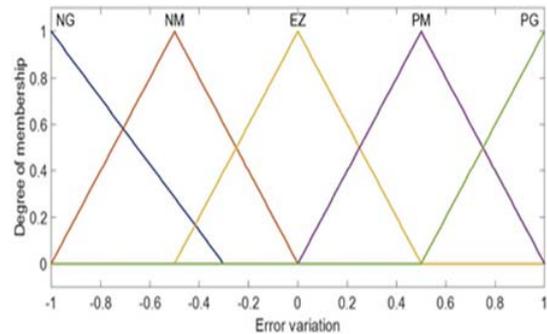
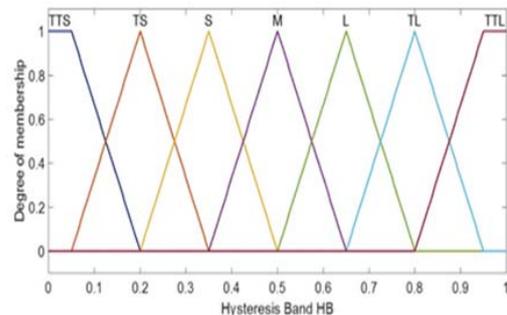Fig.5. Member ship functions for error variation of the real and reactive distorting powers.

Fig.6. Membership function for the output variable HB.

Table 2. Fuzzy inference rule

E \ DE	NTG	NG	NM	EZ	PM	PG	PTG
NG	TTS	TS	S	S	S	M	L
NM	TS	M	L	TL	L	TL	TL
EZ	TTL	TTL	TTL	TTL	TTL	TTL	TTL
PG	TTL	TL	L	TL	TL	L	S
PG	TL	M	S	S	S	TS	TTS

DC voltage control

The role of the DC bus voltage regulation loop is to maintain this voltage at a constant reference value by controlling the capacitor charging and discharging process. The causes of its variation are essentially the losses in the switches of the converter (in conduction and commutation), in the coupling inductors, and the variation of the load connected to the DC bus. This voltage is regulated by

adjusting the amplitude of the references of the sampled currents to control the transit of active power between the network and the DC bus.

To this end, provision is made to compensate for all disturbances on the converter side and the load side, causing a variation in the energy stored in the capacitor. This loop has the reference voltage Vdc* and the measured voltage Vdc as input. [19], [20].

In this case, we will apply two regulators, the classic PI regulator, and an adaptive fuzzy logic PI controller AFLC-PI. Figure 7 shows the DC voltage control configuration using these two regulators.
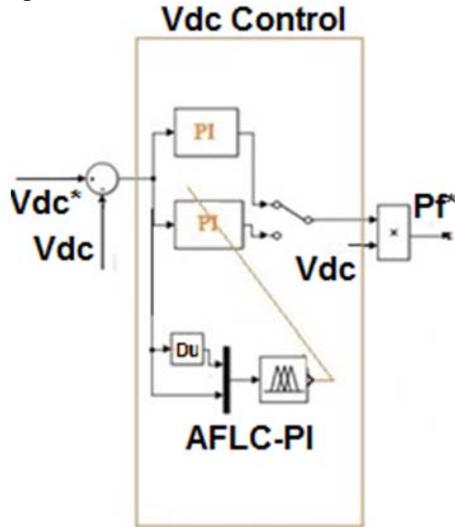
Fig.7..DC voltage control configuration using PI and AFLC-PI.

PI Regulator

A PI-type regulator is often used to control this voltage. By neglecting the active losses in the converter and the coupling inductors, applying the principle of energy conservation gives the ratio between the active power delivered by the network and that received at the output of the bridge. In any case, the dimensioning of PI is well known. Most often, we use the pole placement method [21], [22].

An adaptive fuzzy logic PI controller

The fuzzy control was proven effective when applied alone but also allows the adjustment of existing control parameters. Thus, used research studies show that combining fuzzy logic with traditional commands is even more interesting to make them robust and give rise to robust and straightforward regulators such as, for example, an adaptive fuzzy logic PI controller or AFLC-PI [23]. The proposed AFLC-PI controller is presented in Figure 8.
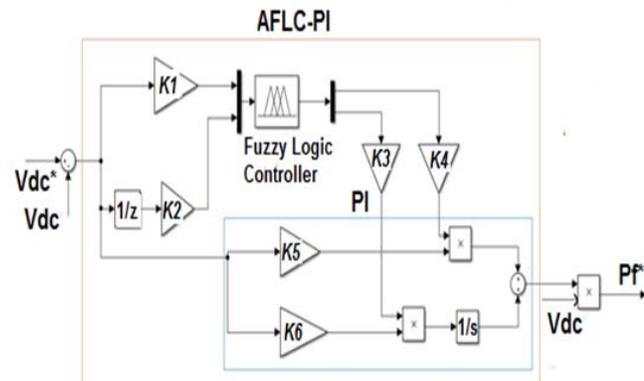
Fig.8. DC voltage control configuration using AFLC-PI.

The control strategy consists in comparing the measured voltage Vdc with the reference voltage Vdc*. This error "e" is considered to be a first input variable, while its derivative "de" is considered to be a second input variable, such as:

(6)
$$e = V_{dc}^* - V_{dc}$$

(7)
$$de(k) = e(k) - e(k-1)$$

Seven fuzzy levels are defined for e and de, which are distributed as follows: large negative (NL), medium negative (NM), small negative (NS), zero (ZR), and small positive (PS), medium positive (PM), and positive large (PL). The outputs variables kpf and kif, the fuzzy parameters, compensate the PI regulators via two normalization gains k4 and k5. With two fuzzy sets labeled small S and big B.
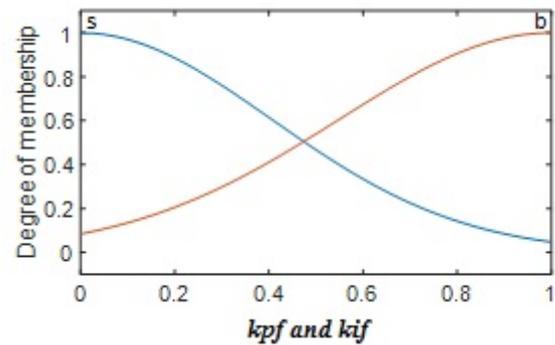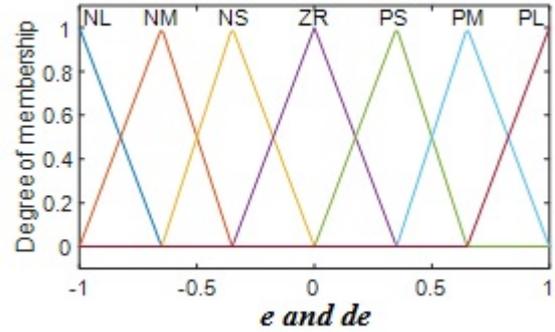
Fig.9. Membership function for the inputs and output variables.

The normalization gains K1 and K2 are used to correct the discourse universe FLC inputs, while K3 and K4 compensate for system errors or disturbances to adapt the PI regulator's initially calculated values K5 and K6. In this case, the min-max inference method was used, and the centroid method was used to deffuzify the fuzzy control variables. The membership functions used for the input and output variables are shown in Figure 8. The fuzzy rule base is given in Table 3.

Table 3. Fuzzy inference rule

de \ e	NL	NM	NS	ZR	PS	PM	PL
NL	B	B	B	B	B	B	B
NM	S	B	B	B	B	B	S
NS	S	S	B	B	B	S	S
ZR	S	S	S	B	S	S	S
PS	S	S	B	B	B	S	S
PM	S	B	B	B	B	B	S
PL	B	B	B	B	B	B	B

Simulations and results

The performance of the proposed controls strategies is evaluated through simulation using Simulink and SimPower Systems toolboxes. The model parameters used for these simulations are listed in Table 4 [20].

Table 4. System parameters

Parameters	Values
Supply voltage	$V_s = 220$ V, $f_s = 50$ HZ
The source side line parameters	$L_s = 0.02$ mH, $R_s = 3.5$ mΩ
Load parameters	$L_{ch} = 0.1$ mH $R_{ch} = 3$ Ω
The load side line parameters	$L_c = 0.02$ mH, $R_c = 3.5$ mΩ
The APF : Interfacing bloc	$L_f = 3$ mH, $R_f = 3$ mΩ
DC bus	$V_{dc} = 700$ V, $C_{dc} = 2.2$ mf
Hysteresis band	H= ± 0.1 A

The following figures show the simulation results of the system illustrated in Fig. 1.

Fig. 10 shows the waveform of the line current absorbed by the nonlinear load consisting of a three-phase rectifier with an RL connection. In Fig. 10, the THD spectrum is presented. It reaches a value of 24.59%.
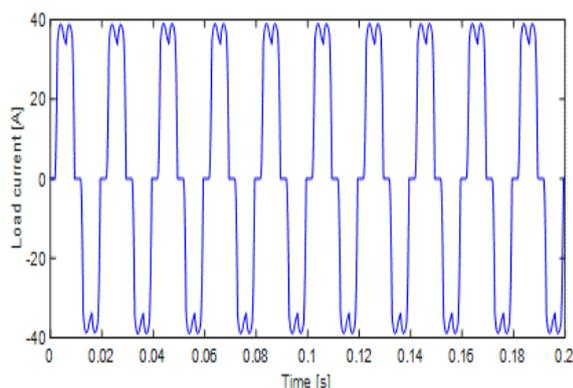
Fig.10. A-phase load current waveform for a nonlinear load consisting of a 3-phase diode bridge rectifier feeding RL load
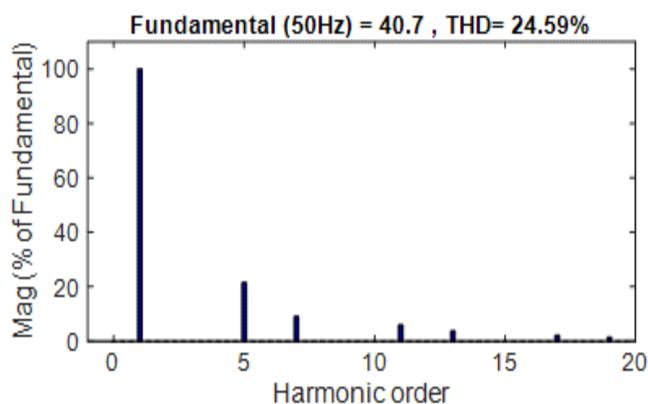
Fig.11. Harmonic spectrum of the load current correspond to the nonlinear load in Fig. 9

To show the efficiency of the active power filter with the different control strategies, we will do four scenarios according to the DC voltage control and the proposed DPC control.

First scenario: in this scenario, a PI and a Direct distorting Power Control (DDPC) control the DC voltage and the APF respectively.
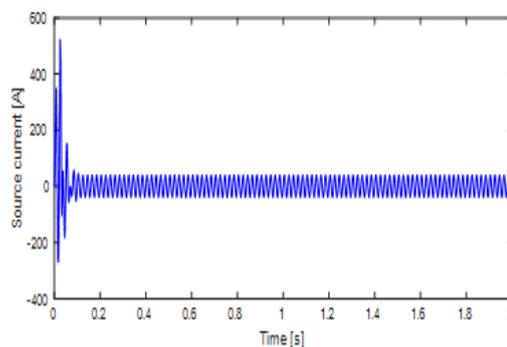
Fig.12. The source current (A)
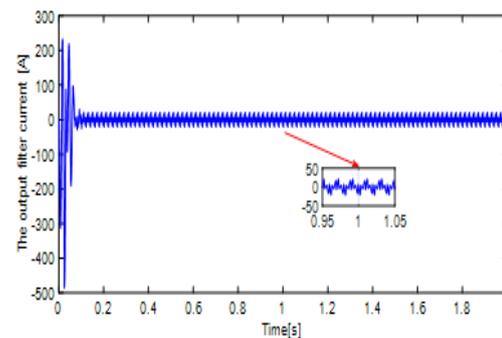
Fig.13. The output filter current (A)
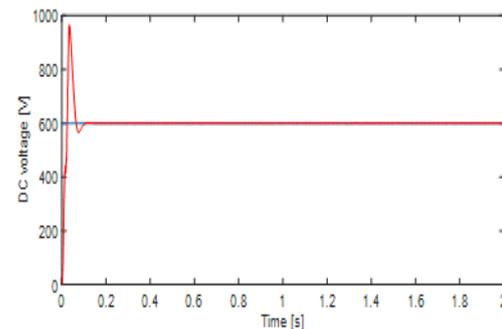
Fig.14. The DC voltage (V)
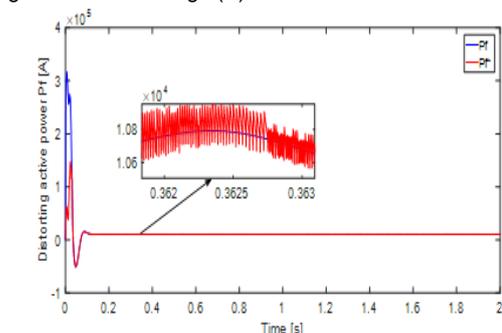
Fig.15. The distorting active power Pf (W).
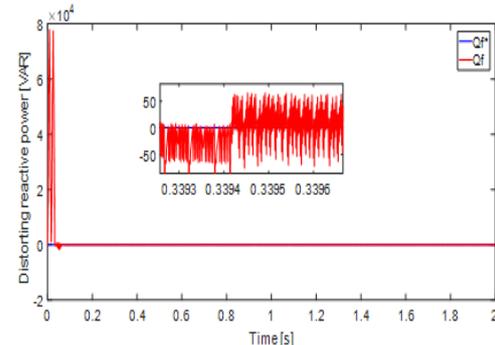
Fig.16. The distorting reactive power Pf (VAR)
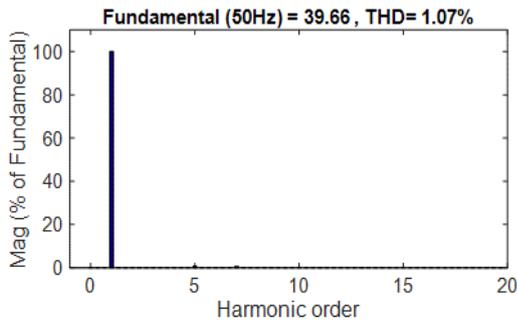
Fig.17. Harmonic spectrum of the source current illustrate in Fig. 11

Second scenario: In this scenario, the DC voltage and the APF are controlled respectively by an AFLC-PI and a Direct distorting Power Control (DDPC).
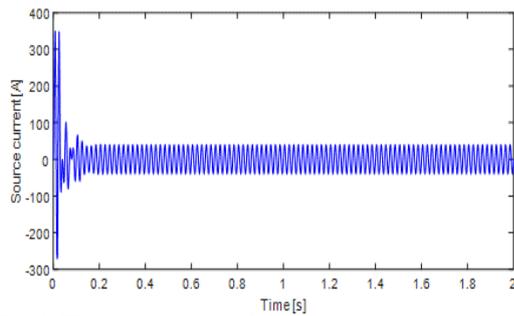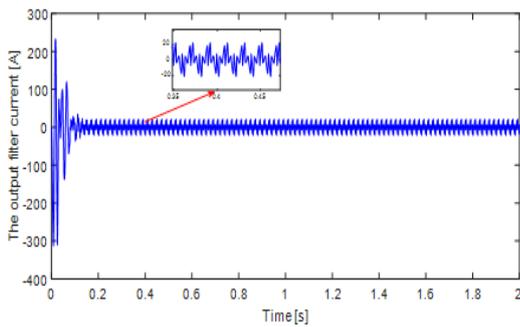

Fig.18. The source current (A)
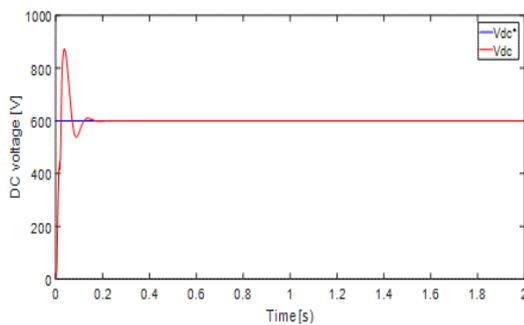

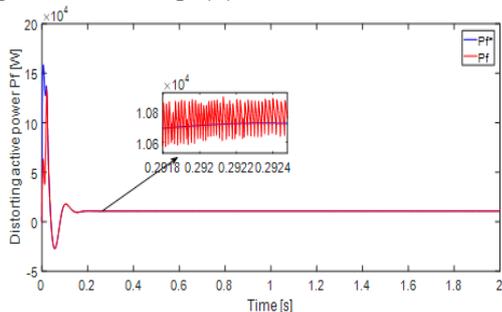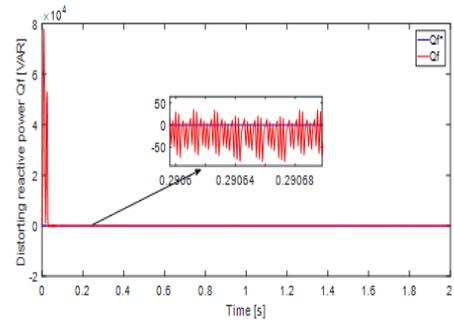Fig.19. The output filter current (A)

Fig.20. The DC voltage (V)

Fig.21. The distorting active power Pf (W)
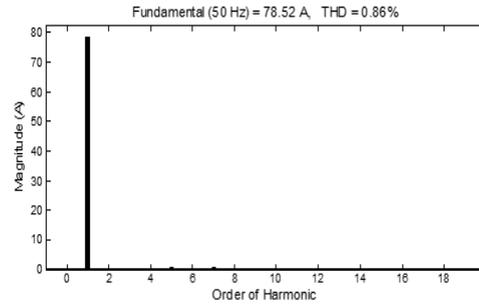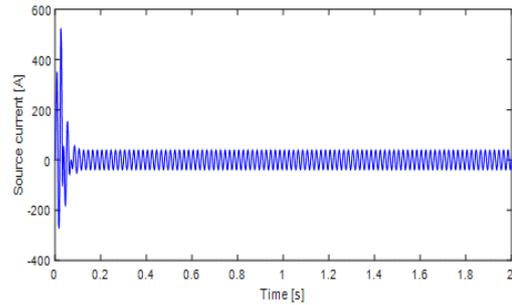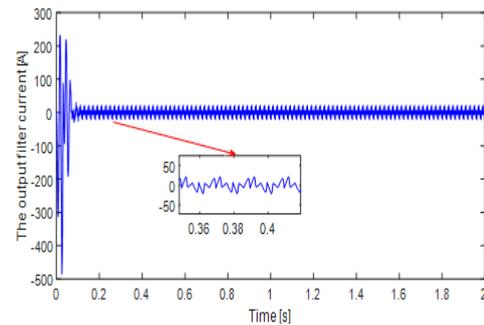

Fig.22. The distorting reactive power Pf (VAR)

Fig. 23. Harmonic spectrum of the source current illustrate in Fig. 17

Third scenario: In this scenario, a PI controls the DC voltage, the APF respectively, and an adaptive fuzzy logic direct distorting power control (AFL-DDPC).

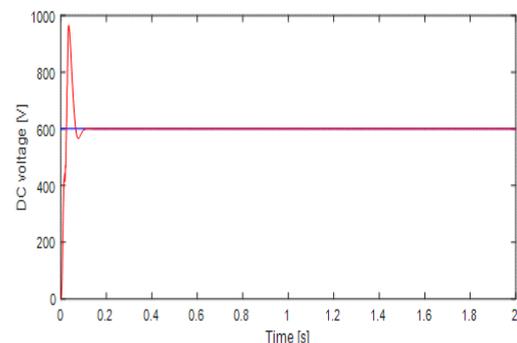Fig.24. The source current (A).

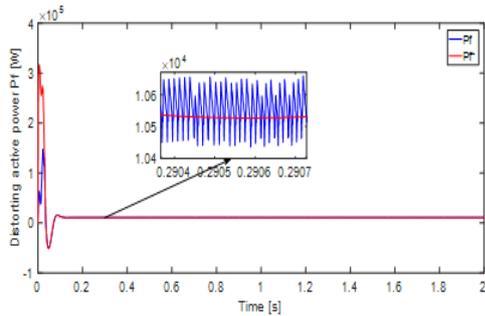Fig.25. The output filter current (A)

Fig.26. The DC voltage (V)

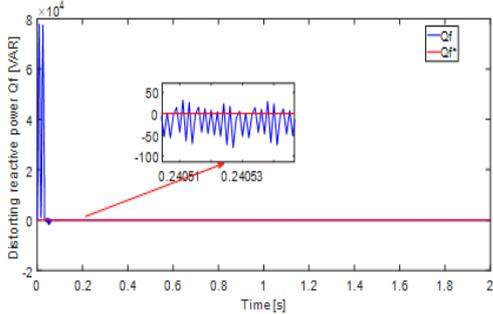Fig.27. The distorting active power Pf (W)

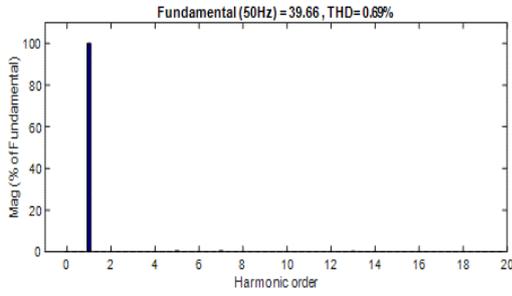Fig.28. The distorting reactive power Pf (VAR)

Fig.29. Harmonic spectrum of the source current illustrate in Fig. 23

Fourth scenario: In this scenario, the DC voltage and the APF are controlled respectively by an AFLC-PI and an adaptive fuzzy logic direct distorting power control (AFL-DDPC).
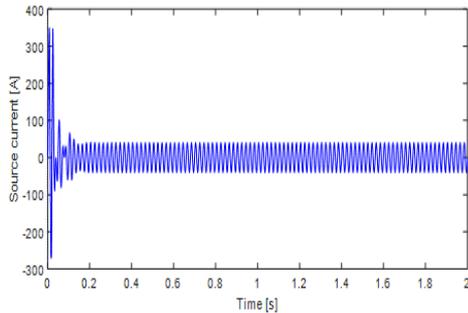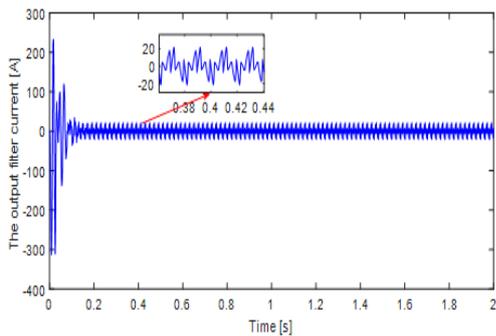

Fig.30. The source current (A)

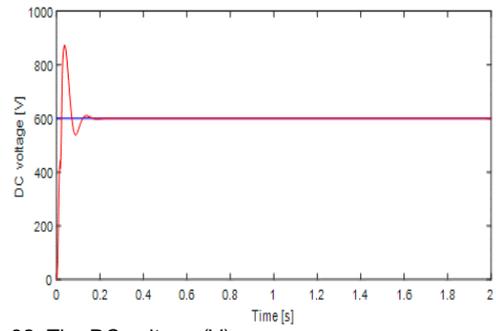Fig.31. The output filter current (A)
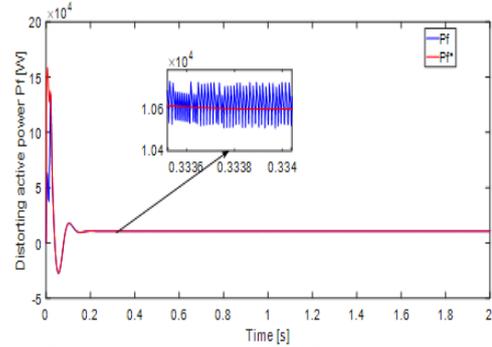

Fig32. The DC voltage (V)

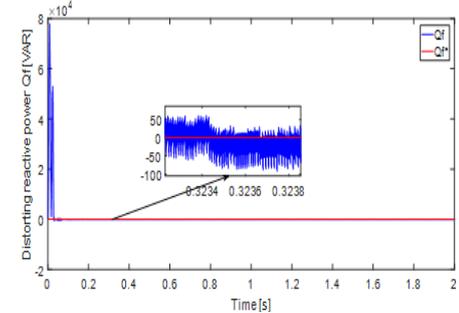Fig.33. The distorting active power Pf (W)

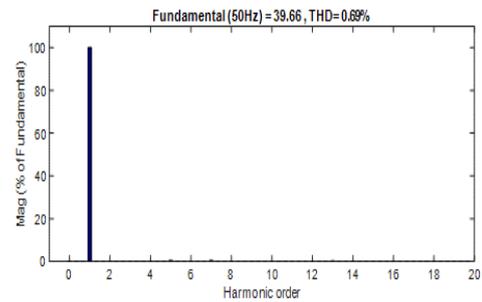Fig. 34. The distorting reactive power Pf (VAR)

Fig.35. Harmonic spectrum of the source current illustrate in Fig. 29

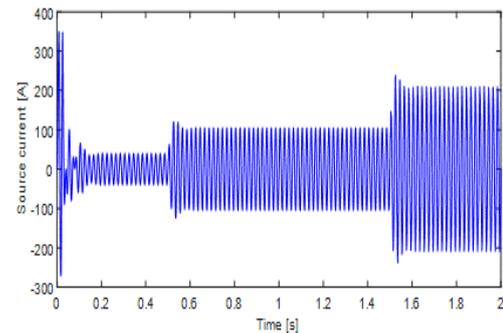**Fifth scenario** : Load variation
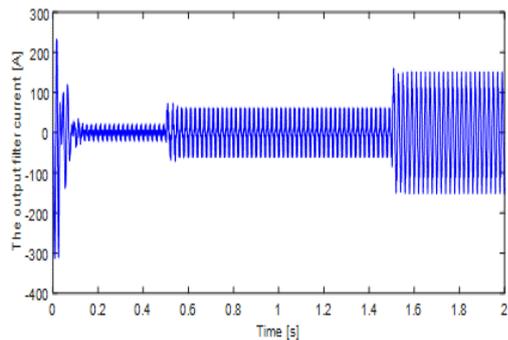

Fig.36. The source current (A)
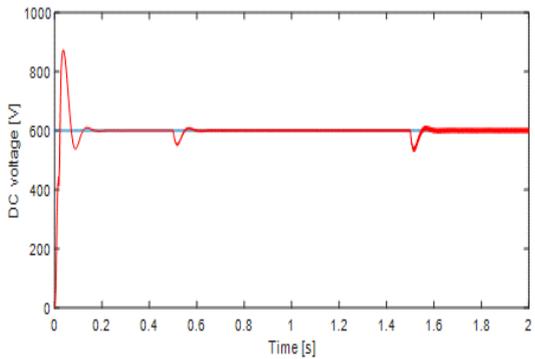
Fig.37. The output filter current (A)
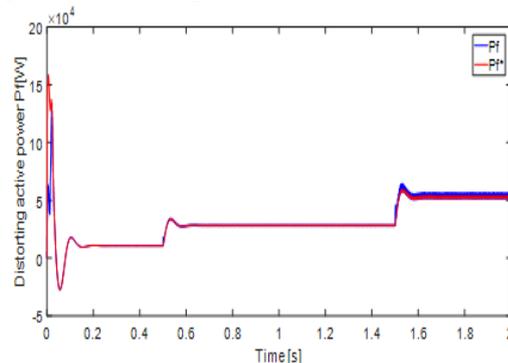

Fig. 38. The DC voltage (V)

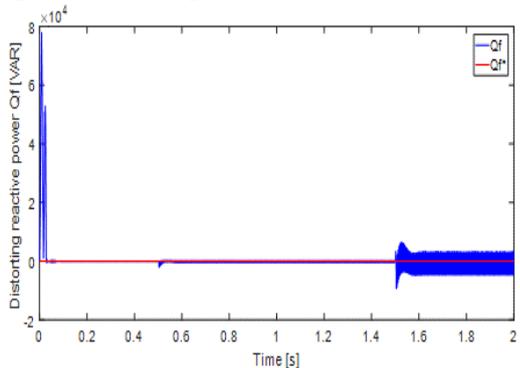Fig.39. The distorting active power P_f (W)

Fig.40. The distorting reactive power P_f (VAR)
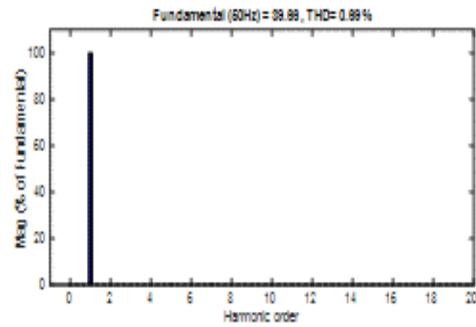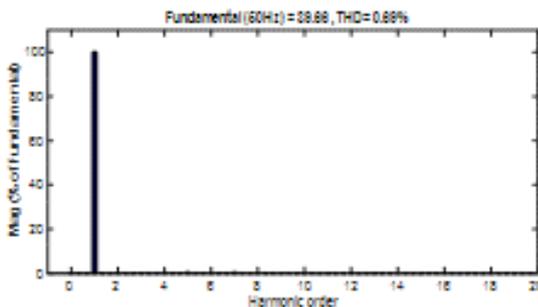
Fig.41. Harmonic spectrum of the source current illustrate in Fig. 35

5.1 Comparison between different controllers

Table 5 shows the response time obtained with the various tuning methods. By observing the results, it can notice that the We can notice that the hybridization between the fuzzy logic and the PI regulator on the DC voltage side on the one hand and with the classic DDPC improves the performance of the active filter in terms of speed, stability, precision and robustness with a better quality of very low harmonic level energy.

Table 5 compares the performance of the different control methods.

Table 5. The performances of different controllers

Vdc Voltage Regulators	DDPC strategies	Peak overshoot in %	Rise time in sec	Settling time in sec	Steady state error	Robustness	THD
PI	DDPC	++	+++	+++	+	-	+
AFLC-PI	DDPC	+	++	++	++	+	+
PI	AFL-DDPC	++	+++	+++	++	++	++
AFLC-PI	AFL-DDPC	+++	+++	+++	+++	+++	+++

Conclusions

The control proposed for SAFP to have the use of the fuzzy controller in two different stages (at the level of the DC bus and the level of the hysteresis controller) has shown its superiority compared to the combination of two classic and intelligent controllers the performance of the active filter with the proposed control is found to be excellent, and the source current is practically sinusoidal. The THD has decreased from 1.45 to 0.82, and finally, the source current is in phase with supply voltage (power factor equal to 1).

Authors: *Pr .Tayeb ALLAOUI , Laboratory of Electrical and Computer Engineering ,university of Tiaret, Algeria*
E-mail: tayeb.allaoui@univ-tiaret.dz.

REFERENCES

[1]   CortÉs, P., RodrÍguez, J., Antoniewicz, P and Kazmierkowski, M. (2008). Direct Power Control of an AFE Using Predictive Control. IEEE Transactions on Power Electronics, vol. 23, no. 5, pp. 2516-2523, doi: 10.1109/TPEL.2008.2002065.
[2]   Bouhouta, A., Moulahoum, s., Kabache, N and Benyamina, A. (2019). Design and Real Time Implementation of Three Phase Shunt Active Power Filter Using Indirect Current Control Technique. International Conference on Advanced Electrical Engineering (ICAEE), pp. 1-6, doi: 10.1109/ICAEE47123.2019.9015096.
[3]   Ismail G., Toufik B.M., Said B. (2018). Real time implementation of feedback linearization control based three phase shunt active power filter, European Journal of Electrical Engineering, Vol. 20, No. 4, pp. 517-532.https://doi.org/10.3166/EJEE.20.517-532
[4]   Madonski, R., Stanković, M., Shao, S., Gao, Z., Yang, J., Li, S. (2020). Active disturbance rejection control of torsional plant with unknown frequency harmonic disturbance, Control Engineering Practice, Vol. 100, 104413, doi.org/10.1016/j.conengprac.2020.104413.
[5]   Wei, G., Zhi-Chao, S., Miroslav, K. (2017). Adaptive rejection of harmonic disturbance anticollocated with control in 1D wave equation, Automatica, V. 79 , pp. 17-26, doi.org/10.1016/j.automatica.2017.01.034.
[6]   Rahmani, R., Hamadi, A., Al-Haddad, K and Dessaint, L. A. (2014). A Combination of Shunt Hybrid Power Filter and Thyristor-Controlled Reactor for Power Quality, IEEE Transactions on Industrial Electronics, vol. 61, no. 5, pp. 2152-2164, doi: 10.1109/TIE.2013.2272271.
[7]   Patjoshi, R. K and Mahapatra, K. K. (2013). Performance comparison of direct and indirect current control techniques applied to a sliding mode based shunt active power filter, Annual IEEE India Conference (INDICON), pp. 1-5, doi: 10.1109/INDCON.2013.6725854.
[8]   Mane, M and Namboothiripad, M. K. (2016). Current harmonics reduction using sliding mode control based shunt active power filter, 10th International Conference on Intelligent Systems and Control (ISCO), pp. 1-6, doi: 10.1109/ISCO.2016.7727005.
[9]   Benyettou, L., Tebbakh, M. (2018). Shunt active filter using fuzzy logic based on three-level (NPC) inverter to compensate current harmonics. Advances in Modelling and Analysis B, Vol. 61, No. 4, pp. 198-206. https://doi.org/10.18280/ama_b.610404
[10]   Loutfi, B. (2019). Comparative analysis hysteresis and fuzzy logic hysteresis controller of shunt active filter. Advances in Modelling and Analysis B, Vol. 62, No. 2-4, pp. 37-42. https://doi.org/10.18280/ama_b.622-401
[11]   Bhende, C. N., Mishra, S and Jain, S. K. (2006). TS-fuzzy-controlled active power filter for load compensation, IEEE Transactions on Power Delivery, vol. 21, no. 3, pp. 1459-1465, doi: 10.1109/TPWRD.2005.860263.
[12]   Mikkili, S., Panda, A. K. (2012). Real-time implementation of PI and fuzzy logic controllers based shunt active filter control strategies for power quality improvement, International Journal of Electrical Power & Energy Systems, Vol. 43, Issue 1, pp. 1114-1126, doi.org/10.1016/j.ijepes.2012.06.045.
[13]   Green, T. C and Marks, J. H. (2005). Control techniques for active power filters, IEE Proc.-Electr. Power Appl., Vol. 152, No. 2, pp. 369-381
[14]   Antoniewicz, P and Kazmierkowski, M. P. (2008). Virtual-Flux-Based Predictive Direct Power Control of AC/DC Converters With Online Inductance Estimation, IEEE Transactions on Industrial Electronics, vol. 55, no. 12, pp. 4381-4390, doi: 10.1109/TIE.2008.2007519.
[15]   Ge, J., Zhao, Z., Yuan, L., Lu, T and He, F. (2015). Direct Power Control Based on Natural Switching Surface for Three-Phase PWM Rectifiers, IEEE Transactions on Power Electronics, vol. 30, no. 6, pp. 2918-2922, doi: 10.1109/TPEL.2014.2377048.
[16]   Portillo, R., Vazquez, S., Leon, J. I., Prats, M. M and Franquelo, L. G. (2013). Model Based Adaptive Direct Power Control for Three-Level NPC Converters, IEEE Transactions on Industrial Informatics, vol. 9, no. 2, pp. 1148-1157, doi: 10.1109/TII.2012.2209667.
[17]   Jiang, Z., Chang, Y., Qingru, Q., Zheng,Y., Yixin, N., Zhang, B. I., Shousun, C., Felix, F. W. (2004). A novel hysteresis current control for active power filter with constant frequency, Electric Power Systems Research, Vol. 68, Issue 1, pp. 75-82, doi.org/10.1016/S0378-7796(03)00158-5.
[18]   Fereidouni, A., Masoum, M. A. S and Smedley, K. M. (2016). Supervisory Nearly Constant Frequency Hysteresis Current Control for Active Power Filter Applications in Stationary Reference Frame, IEEE Power and Energy Technology Systems Journal, vol. 3, no. 1, pp. 1-12, doi: 10.1109/JPETS.2015.2501423.
[19]   Guentri, H., Allaoui, T., Mekki, M., Denai, M. (2021). POWER management and control of A PHOTOVOLTAIC system with hybrid battery-supercapacitor energy storage BASED ON HEURISTICS METHODS, Journal of Energy Storage, Vol. 39, 102578, doi.org/10.1016/j.est.2021.102578.
[20]   Kouadria, M. A., Allaoui, T., Belfedal, C. (2014). A Fuzzy Logic Controller of Three-Phase Shunt Active Filter for Harmonic Current Compensation, International Journal of Advances in Engineering & Technology (IJAET), Vol. 7 Issue 1, pp. 82-89
[21]   Larrinaga, S. A., Vidal, M. A. R., Oyarbide, E and Apraiz, J. R. T. (2007). Predictive control strategy of DC/AC converters based on direct power control, IEEE Trans. on Industrial Electronics, vol. 54, no. 3, pp. 1261-1271
[22]   Bouafia, A., Krim, F., Gaubert, JP. (2009). Design and implementation of high performance direct power control of three-phase PWM rectifier, via fuzzy and PI controller for output voltage regulation, Energy Convers Manage, vol. 50, no.1, pp.6–13
[23]   Faiza, A.A., Morsli, S., Tayeb, A. (2020). Self tuning filter based fuzzy logic controller for active power filter. Journal Européen des Systèmes Automatisés, Vol. 53, No. 5, pp. 739-745. https://doi.org/10.18280/jesa.530517